Orientation and Dynamics of Phospholipid Head Groups in Bilayers and Membranes Determined from ^{31}P Nuclear Magnetic Resonance Chemical Shielding Tensors†

Susan J. Kohler* and Melvin P. Klein

ABSTRACT: ^{31}P nuclear magnetic resonance (NMR) powder spectra have been used to determine the principal values of the chemical shielding tensors of phosphatidylcholine, phosphatidylethanolamine, phosphatidylserine, and phosphatidic acid. The shielding tensors in all cases were clearly nonaxial. The principal values for the monoester phosphatidic acid shielding tensor are −40, −4, and 48 ppm relative to 85% H_3PO_4. By contrast the diesters have values of −87, −25, and 119 ppm for phosphatidylcholine, −81, −20, and 105 ppm for phosphatidylethanolamine, and −80, −20, and 112 ppm for phosphatidylserine. This difference reflects the sensitivity of the ^{31}P shielding tensor to chemical environment. Anisotropic motion of the molecules in lamellar dispersions of phospholipids caused an incomplete averaging of the shielding tensors resulting in partially narrowed spectra. Spectra of various phospholipid dispersions were recorded as a function of temperature and transitions observed at the gel–liquid crystalline phase transition temperatures. Using a reasonable set of initial conditions, it was shown that a simple model of molecular motion could successfully predict the observed spectra and their temperature dependences. The model includes rotations about the P–O(glycerol) bond and the molecular z axis and a wobble of the molecule about the bilayer normal. As the temperature increases, the wobble amplitude increases and the spectra narrow. A preliminary ^{31}P NMR spectrum of chick embryo fibroblasts is included. The similarities between this spectrum and those of the lamellar dispersions indicate that some of the predominant features are due to the phospholipid resonances.

The polar head groups of phospholipids are of interest due to their biological significance in the determination of the properties of both phospholipid dispersions and biological membranes. The importance of the head groups is reflected in the specific phospholipid requirements of various membrane-bound enzymes (Steck and Fox, 1972), as well as the variation of phospholipid head-group composition which occurs from organelle to organelle and species to species (Rouser et al., 1968). Modification of the head groups is known to cause changes in the cooperative properties of bilayer dispersions. The fluidity of phospholipid dispersions is sensitive to the type of head group present; the thermal phase transition (Chapman transition) from the gel to liquid crystalline state is significantly higher for DPPE[1] than for DPPC (Chapman, 1975). The fluidity is also sensitive to head-group perturbants such as pH and Ca^{2+} concentration (Verkleij et al., 1974) and it has been shown that Ca^{2+} introduces lateral phase separation in mixed phospholipid dispersions (Jacobson and Papahadjopoulos, 1975). Similar cooperative interactions in biological membranes might be involved in cellular response to drugs and anesthetics (Chapman, 1975). For these reasons it is of considerable interest to determine the dynamic properties of the phospholipid head groups in membrane and model membrane systems.

The properties of the polar head groups have been studied by a variety of physical techniques including x-ray crystallography, fluorescence spectroscopy, electron spin resonance spectroscopy (ESR), and nuclear magnetic resonance spectroscopy (NMR). X-ray crystallography has given detailed information about the geometry of phospholipids and their component parts but is inherently restricted to their static conformations. Fluorescence and ESR spectroscopy have provided information of a dynamic nature but have the disadvantage of the introduction of a perturbing reporter group into the molecule. Most NMR has been done using the ^{1}H and ^{13}C nuclei where dynamic information is available from the analysis of T_1 and T_2 relaxation time data, but this analysis is not straightforward due to the possibility of several competing relaxation mechanisms (Horwitz et al., 1973; Stockton et al., 1976; Seelig and Seelig, 1974a). More direct dynamic information is attainable from analysis of the quadrupolar splittings in ^{2}H spectra and the chemical shift anisotropies in ^{31}P and ^{13}C spectra. These interactions are anisotropic and are only partially averaged when the molecules undergo restricted motion, and analysis of the spectra may give direct information on the nature of this motion.

Unsonicated phospholipid dispersions and biological membranes are systems in which ^{31}P chemical shift anisotropies are observed, and these residual anisotropies may be analyzed in terms of the molecular motions if the principal values and orientations of the rigid lattice chemical shielding tensors are known.

In this paper we report values for the elements of the chemical shielding tensors of a variety of phospholipids determined from ^{31}P NMR spectra of phospholipid powders. These tensors are then used to interpret the spectra from la-

† From the Laboratory of Chemical Biodynamics, Lawrence Berkeley Laboratory, University of California, Berkeley, California 94720. *Received June 28, 1976.* This research was supported in part by the United States Energy Research and Development Administration and in part by the National Cancer Institute (Grant CA 14828). S.J.K. is a Postdoctoral Fellow of the National Cancer Institute of the National Institutes of Health (Grant 1F22 CA01269-01).

[1] Abbreviations used: PA, phosphatidic acid; PC, phosphatidylcholine; PE, phosphatidylethanolamine; PS, phosphatidylserine; DSPA, distearoylphosphatidic acid; DPPC, dipalmitoylphosphatidylcholine; DPPE, dipalmitoylphosphatidylethanolamine; NMR, nuclear magnetic resonance; ESR, electron spin resonance; TLC, thin-layer chromatography; EDTA, ethylenediaminetetraacetic acid.

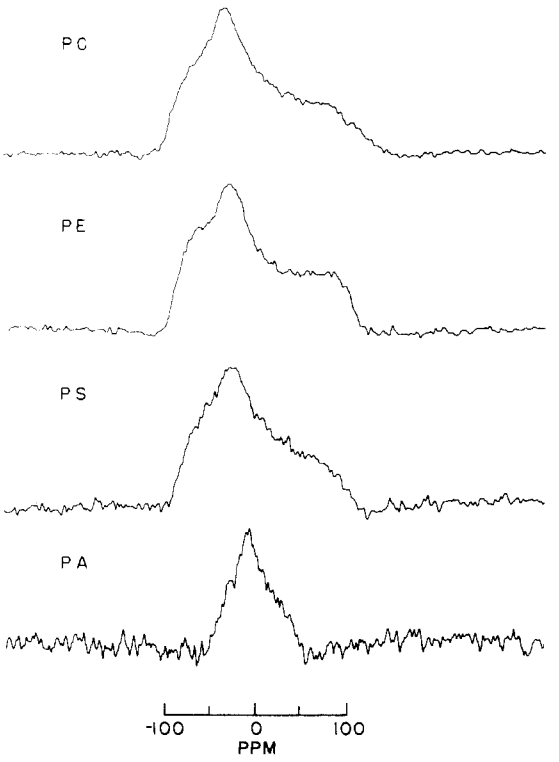

FIGURE 1: ^{31}P NMR spectra of phospholipid powders taken at 24 MHz in the presence of 60 MHz ^1H decoupling field. The scale takes the resonance of 85% H_3PO_4 as 0 ppm and assigns resonances at lower fields negative values.

mellar phospholipid dispersions, and a possible simple model of the molecular dynamics of the phospholipids in these dispersions is developed. We conclude with preliminary observations of the ^{31}P resonances from chick embryo fibroblasts.

Experimental Section

Sample Preparation. DPPC and DPPE were obtained from Sigma, DSPA from Applied Science Labs, and brain extract (type III) from Sigma. Anhydrous samples of DPPC and DPPE were prepared by drying the compounds under a vacuum of approximately 1 μm at a temperature of 85–95 °C for at least 5 h. This was done in the presence of a liquid-nitrogen trap, and the samples were sealed before removal from the vacuum line. Egg PC was extracted from hen egg yolks by the method of Singleton (1965) and stored in ethanolic solution under Ar in a freezer. All samples except brain extract were found to be chromatographically pure by TLC on silica gel (Adsorbosil-5, Applied Science Labs) eluted with $CHCl_3$–MeOH–H_2O (130:50:4 v/v/v) or $CHCl_3$–MeOH–H_2O–HAc (25:15:2:4 v/v/v/v). The brain extract reportedly contained 80–85% PS, 5–10% cerebrosides, and 5% PA, and this was qualitatively supported by the TLC results.

Lamellar dispersions of the phospholipids were formed by mixing 100 mg of phospholipid with 0.5–1.0 ml of borate buffer at pH 7.4 (0.08 M H_3BO_3–0.002 M $Na_2B_4O_7$–0.08 M NaCl–0.0001 M EDTA) for PC and brain extract and with 0.5–1.0 ml of borate buffer at pH 11.4 (0.015 M $Na_2B_4O_7$–0.04 M NaOH–0.0001 M EDTA) for PE. Two glass beads were added to the mixture in a 25-ml flask; the flask was flushed with Ar and sealed and shaken by hand in a hot water bath until the dispersion formed. Although the buffer/phospholipid ratio varied, it was always sufficient to ensure full mobility of the phosphate head groups (Veksli et al., 1969; Griffin, 1976) and the formation of lamellar dispersions (Chapman et al., 1967).

A brain extract sample was prepared for electron microscopy by dispersing 100 mg of brain extract in 0.7 ml of ammonium acetate buffer (0.2 M $NH_4C_2H_3O_2$–0.006 M NH_4OH) at pH 7.4 and then diluting it 25-fold with buffer and staining the diluted sample with 2% ammonium molybdate after the method of Papahadjopoulos (1967). The electron micrographs showed a distribution in particle diameter ranging from 0.25 to 0.75 μm.

Secondary cultures of chick embryo fibroblasts were prepared as previously described (Bissell et al., 1974; Rein and Rubin, 1968) and incubated 2 days before harvesting. The cells were removed by trypsinization, washed three times in physiological saline solution, and pelleted in a clinical centrifuge at 1500 rpm for 15 min. The supernatant was decanted and the cells were packed into an NMR tube.

NMR Equipment and Techniques. ^{31}P spectra were taken either by the cross-polarization technique (Pines et al., 1973) or by the simple decoupling technique as described previously (Kohler and Klein, 1976) using a home-built 24.3-MHz spectrometer described in detail elsewhere (Kohler et al., 1976). The inclusion of 30-MHz cutoff filters before the preamplifier diodes and on the probe side of the transmitter diodes improved the signal-to-noise ratio by a factor of 20 during double-resonance operation. The replacement of the simple pulse sorter with a programmable pulse generator greatly enhanced the ease of operation.

Temperature control was achieved by flowing a stream of heated or cooled nitrogen past the sample. The probe temperature was measured with a thermocouple placed in a water-filled NMR tube in place of the sample, and the apparatus was adjusted in the presence of the rf pulses to the desired steady-state temperature. The temperature was checked before and after each spectrum and typically varied less than 1 °C for the spectra taken above 0 °C and less than 3 °C for the spectra taken below 0 °C. The same sample was used for all spectra taken in the course of a temperature run. After completion of the temperature studies, spectra were taken again at room temperature and compared with the original room temperature spectra to verify that no irreversible changes occurred as a result of the heating or cooling.

The values of the principal elements of the chemical shielding tensors were determined by matching computer simulated spectra with the experimental spectra of the phospholipid powders. The same procedure was used to obtain the reduced tensor elements from the spectra of the lamellar dispersions.

Results

^{31}P cross-polarization spectra of the phospholipid powder samples appear in Figure 1 and the values of the principal elements of the shielding tensors obtained from these spectra are given in Table I. In all cases the shielding tensors are clearly nonaxial. The spectra of DPPC, DPPE, and brain extract (PS)[2] are very similar, while that of PA is noticeably different. This is not surprising since the former compounds are all diesters and are identical in structure within a range of at least three

[2] The small amounts of lipids other than PS are believed to be insignificant in their contribution to the spectra, and therefore the brain extract spectra are considered to be spectra of PS. For this reason, we refer to brain extract as "brain extract (PS)".

TABLE I: ^{31}P Chemical Shielding Tensors of Phospholipids.[a]

	DPPE			DPPC				Brain (PS)			DSPA		
	σ_{11}	σ_{22}	σ_{33}	σ_{11}	σ_{22}	σ_{33}		σ_{11}	σ_{22}	σ_{33}	σ_{11}	σ_{22}	σ_{33}
Powder	−81	−20	105	−87	−25	119	EGG PC	−80	−20	112	−40	−4	48
Lamellar Dispersion (at specified temp, °C)	$\sigma_\perp$	$\sigma_\parallel$		$\sigma_\perp$	$\sigma_\parallel$		$\sigma_\perp$	$\sigma_\parallel$	$\sigma_\perp$	$\sigma_\parallel$			
−29							20	−47					
−14							17	−27	16	−56			
13				20	−39		17	−26	15	−27			
27	18	−34		20	−36		15	−28	14	−30			
37	16	−36		17	−35								
44	17	−32		16	−27								
55	16	−32		15	−26		13	−23	14	−26			
64	9	−19		15	−24								
74	6	−10											

[a] The rigid lattice values are taken from spectra of powder samples. The uncertainty is estimated as ± 4 ppm. As explained in the text, these values are partially averaged in the spectra of multilamellar dispersions due to the presence of molecular motion. The values of the averaged tensors are given for phospholipid dispersions at various temperatures, and these data are plotted in Figure 3. All values are in ppm relative to 85% H_3PO_4. The rigid lattice values for DPPC and DPPE are more accurate than those previously reported (Kohler and Klein, 1976) due to the improved sensitivity now available, and the DPPC values are within approximately 10% of those reported by Griffin (1976).

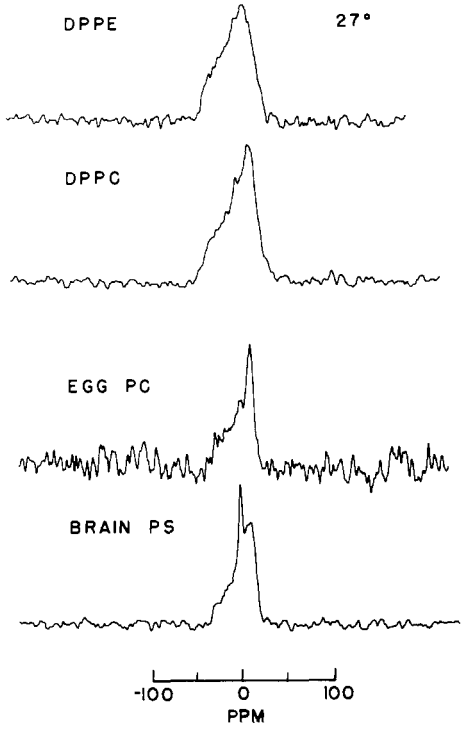

FIGURE 2: ^{31}P NMR spectra of lamellar dispersions of phospholipids taken under the same conditions as those in Figure 1. The samples had a phospholipid/buffer ratio of 1:5–1:10 (w/w), as explained in the text. The spectra all show a collapse to the shapes expected for axially symmetric shielding tensors resulting from molecular motion.

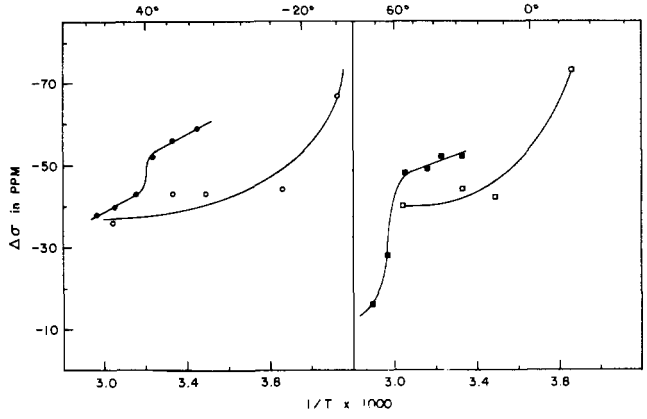

FIGURE 3: $\Delta\sigma$ as a function of inverse temperature for various phospholipid lamellar dispersions, DPPC (●); egg PC (○); DPPE (■); brain PS (□). $\Delta\sigma$ is defined as $\sigma_\parallel - \sigma_\perp$ and was obtained from spectra such as those of Figure 2. A tabulation of these values is given in Table I.

atoms of the phosphorus, while the latter is a monoester and therefore differs from the diesters at the second atom from the phosphorus nucleus. The DPPE and DPPC spectra in Figure 1 are virtually identical with spectra we obtained with anhydrous DPPE and DPPC and indicate that these samples initially had very low water content (Griffin, 1976).

Figure 2 presents ^{31}P free induction decay spectra of unsonicated lamellar dispersions of phospholipids in borate buffer. The spectra all show a collapse to the pattern characteristic of axially symmetric shielding tensors.[3] The residual anisotropies, $\Delta\sigma$, are 40–50 ppm in contrast with the rigid lattice values of 150–200 ppm for these compounds. This collapse is indicative of averaging of the shielding tensors due to motion of the phosphate head groups. Similar spectra were taken as a function of temperature, and the residual anisotropies are plotted as a function of inverse temperature in Figure 3. The DPPC and DPPE samples have discontinuities in $\Delta\sigma$ at their Chapman temperatures, the temperatures associated with the gel to liquid crystal phase transitions. Similar results have been reported previously for sonicated (DeKruijff et al., 1975; McLaughlin et al., 1975a) and unsonicated (Cullis et al., 1976; Gally et al., 1975) preparations of DPPC and for

[3] The spectra of brain extract (PS) dispersions usually had a sharp resonance centered at 0 ppm superimposed on a broader resonance. This sharp peak is believed to be due to the presence of small, rapidly tumbling vesicles existing individually or as the innermost layers of the lamellae, and this peak was ignored when determining $\Delta\sigma$. It is not believed to be due to the other phospholipids in the brain extract since the spectra of dispersions of PS alone also have this peak.

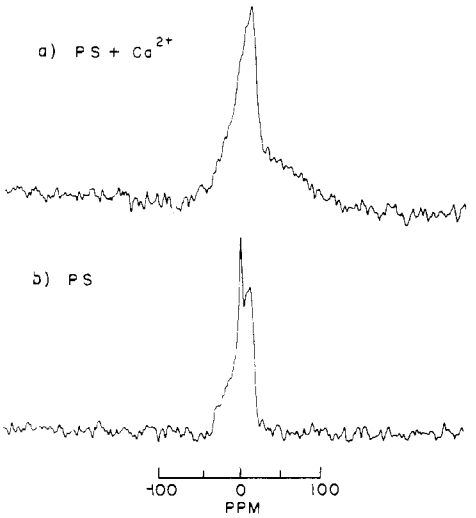

FIGURE 4: Spectra of PS dispersions in the presence and absence of Ca^{2+}. Again, the spectra were taken under the conditions used for those of Figure 1. Trace a is of a PS dispersion formed in the presence of Ca^{2+} in the ratio of 2 Ca^{2+}/PS. This spectrum shows a marked broadening attributed to immobilized PS phosphate, as explained in the text.

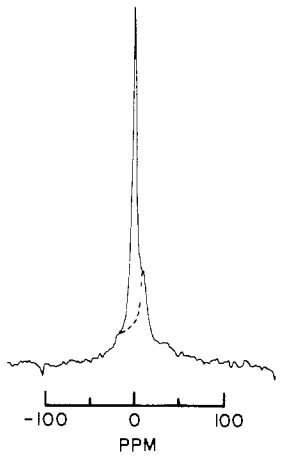

FIGURE 5: ^{31}P NMR spectrum of chick embryo fibroblasts. The spectrum was taken under the same conditions used for the spectra of Figure 1. The narrow resonance centered at 0 ppm is attributed to intracellular phosphate, while the broader resonance is believed due to membrane phospholipids. The dashed line is included to suggest the probable shape of the broad resonance.

unsonicated DPPE (Seelig and Gally, 1976). The data in Figure 3 reflect the head-group motion; yet transitions are seen at temperatures usually associated with the melting of the hydrocarbon tails. It is interesting that DPPE and DPPC differ only in their head groups and yet their transition temperatures differ by approximately 20 °C. The other two dispersions studied, those of egg PC and brain extract (PS), also show discontinuities in their $\Delta\sigma$ behavior. In these cases, the transitions occur at lower temperatures and extend over a wider temperature range. This is characteristic of the Chapman transitions of dispersions of natural phospholipids which typically contain a mixture of saturated and unsaturated fatty acids in their hydrocarbon tails.

Ca^{2+} in borate buffer was added to a brain extract (PS) dispersion in quantity sufficient to have a nominal Ca^{2+}/P molar ratio of 2/1. The ^{31}P NMR spectrum of this mixture is shown in Figure 4, along with that of a similar brain extract (PS) dispersion with no added Ca^{2+}. The spectrum of the dispersion with calcium ions has a resonance typical of phospholipid lamellae superimposed on a much broader peak. The width of the broad resonance is approximately that of the PS rigid lattice width and suggests the presence of immobilized phospholipid head groups.

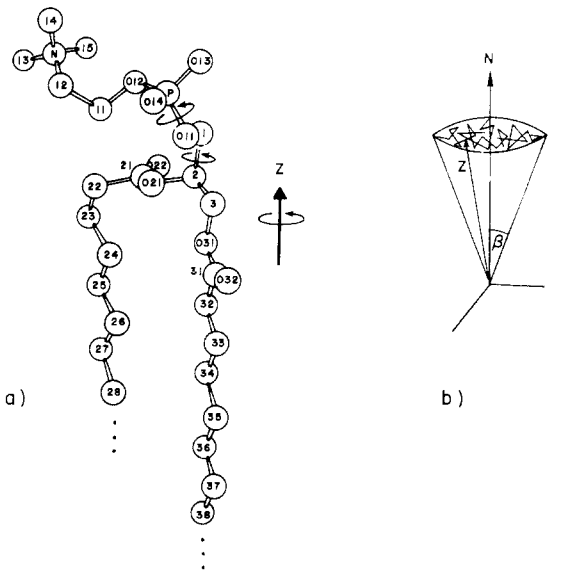

FIGURE 6: Motions used in the formulation of the model of head-group motion. A truncated DPPC molecule is drawn in a and the rotations about P-O11, C1-C2, and the molecular z axis are indicated. Rotation about O11-C1 was also considered, but could not be shown on the figure. The labeling of the atoms is consistent with that used in the x-ray crystallographic work on dilauroyl-PE (Hitchcock et al., 1974). The wobble motion is schematically drawn in b. The molecular z axis executes a random walk within a cone centered on the bilayer normal N. Variation of the angle β changes the area over which z may execute the walk.

Figure 5 contains a ^{31}P spectrum of chick embryo fibroblasts. The spectrum is the superposition of a narrow peak centered at 0 ppm and a broader resonance with a shape typical of the resonances of phospholipid dispersions. The narrow resonance is believed due to relatively small intracellular molecules, while the broader asymmetric resonance is attributed to the membrane phospholipids.

Discussion

Order parameters are commonly used to describe the orientation or molecular motion of quadrupolar nuclei in molecules which are undergoing anisotropic motion. The NMR spectra of such nuclei contain multiplets in place of the single resonances seen for isotropically tumbling molecules. These quadrupolar splittings are caused by the interaction between the nuclear and electronic charge distributions and depend on the nuclear spin, the symmetry of the electric field gradient at the nucleus, and the orientation of the molecule in the external magnetic field. ^2H nuclei (spin = 1) in an axially symmetric field gradient will have a quadrupolar splitting of

$$\Delta\nu = \frac{3}{4}(e^2qQ/h)S(3\cos^2\theta - 1)$$

where e, q, Q, and h have their usual meanings and θ is the angle between the motional averaging axis fixed on the molecule and the direction of the external magnetic field. If the sample is a powder, the θ dependence causes the well-known Pake line shape and the order parameter S is measurable directly from the observed splitting. S, in turn, is defined by

$$S = \left\langle \frac{3\cos^2\alpha - 1}{2} \right\rangle$$

TABLE II: Orientation Information Used in Calculating the Averaged Chemical Shielding Tensors.[a]

Axis (R)	θ	Ψ	γ_1	γ_2	γ_3	γ_4
(R1) P-O11	87.80	36.47		67.73	30.24	150.20
(R2) O11-C1	40.07	86.53	67.73		74.61	90.01
(R3) C1-C2	69.04	58.50	30.24	74.61		161.25
(R4) Molecular z	58.72	−51.68	150.20	90.01	161.25	

[a] The principal axis system of the shielding tensors was taken such that the z axis was along the molecular O13-O14 direction and the x axis was taken along the O11-O12 direction. θ and Ψ are Euler angles of R in the principal axis system of the tensor. γ_1 is the angle between R and P-O11, γ_2 is the angle between R and O11-C1, γ_3 is the angle between R and C1-C2, and γ_4 is the angle between R and the molecular z axis.

where α is the angle between the motional averaging axis and the principal axis of the electric field gradient tensor and the bracket denotes an average over the experimental time scale. The value of the order parameter S depends on the average orientation of the axis of motional averaging with respect to the electric field gradient axis and a change in the value of S will reflect either a change in α from one fixed value to another or a change in the range over which α fluctuates. A priori one cannot distinguish between the two cases, and an interpretation of the order parameter as a measure of "fluidity" or "freedom of motion" must be made cautiously (Seelig and Seelig, 1974a). An additional difficulty occurs if the motional axis is parallel to the electric field gradient axis, for if $\alpha = 0$, then $S = 1$, and there is no indication that the molecule is undergoing motion.

In the case of an axial chemical shielding tensor, there is only one definable independent axis and an order parameter approach similar to that used for quadrupolar splittings is appropriate. If the shielding tensor is nonaxial, as is the case for phospholipids, there are two independent axes and the simple single order parameter approach is neither correct nor appropriate. The dependence of the spectrum on the nature of the motion may be calculated in a straightforward manner by transforming the chemical shielding tensor from its principal axis system to a reference system based on the motional averaging axis, and then averaging the tensor over the motion (Van et al., 1974). If more than one motion is present, sequential transformations and averages may be performed if the motions are independent and the averages are performed over the temporal hierarchy of motion.

Rotation about a single fixed axis averages the initial shielding tensor to one which is axially symmetric and has the components

$$\bar{\sigma}_\perp{}^R = \frac{\sigma_{11}}{2}(\cos^2\theta\cos^2\psi + \sin^2\psi) + \frac{\sigma_{22}}{2}(\cos^2\theta\sin^2\psi + \cos^2\psi) + \frac{\sigma_{33}}{2}\sin^2\theta \quad (1a)$$

$$\bar{\sigma}_\parallel{}^R = \sigma_{11}\sin^2\theta\cos^2\psi + \sigma_{22}\sin^2\theta\sin^2\psi + \sigma_{33}\cos^2\theta \quad (1b)$$

where σ_{11}, σ_{22}, and σ_{33} are the principal elements of the shielding tensor and θ and ψ are Euler angles of the rotation axis in the principal axis frame of the shielding tensor.

Averaging over a second rotation axis further reduces the averaged tensor to

$$\bar{\sigma}_\perp{}^{R_1R_2} = \frac{1}{2}\{\bar{\sigma}_\perp{}^R(\cos^2\gamma + 1) + \bar{\sigma}_\parallel{}^R\sin^2\gamma\} \quad (2a)$$

$$\bar{\sigma}_\parallel{}^{R_1R_2} = \bar{\sigma}_\perp{}^R\sin^2\gamma + \bar{\sigma}_\parallel{}^R\cos^2\gamma \quad (2b)$$

where γ is the time-independent angle between the two axes of rotation; additional rotations may be treated by the repeated use of eq 2a and 2b.

In analyzing the motion of the phosphates of the lamellar dispersions, we considered the P-O11, O11-C1, C1-C2, and z axis rotations diagrammed in Figure 6a as those most likely to affect the phosphate motion, and further we assumed that the total motion was a composite of simple rapid rotations occurring independently on different time scales. It is obvious that many more intricate types of motion (i.e., coupled rotations or oscillations) may be imagined for a system as complex as phospholipid lamellae. It is nevertheless instructive and informative to determine whether a *simple* model of uncoupled rotations will suffice to predict the observed spectra.

In order to proceed with the analysis, it is necessary to know the orientations of the rotation axes with respect to the shielding tensor reference frame. This information is not directly available at the present time, but a reasonable approximation may be made on the basis of existing data. First we assume the orientations of the chemical shielding tensors are the same as those found for phosphorylethanolamine (Kohler and Klein, 1976) and serine phosphate (Kohler and Klein, unpublished data). The most downfield component of the tensor is in the (C)O-P-O(C) plane and the most upfield component of the tensor is in the perpendicular O-P-O plane. We deem this assumption warranted by the similarities of the compounds as discussed elsewhere (Kohler and Klein, 1976). We then use the orientation of the phosphate in crystalline dilauroyl-PE (Hitchcock et al., 1974) to relate the possible rotation axes to the shielding tensor reference frame. The orientation of the phosphate in crystalline PE is used because it is the best approximation available for the phosphate orientation in the phospholipid lamellae.[4] The orientations of the possible rotation axes with respect to the shielding tensor reference frame calculated from these data are summarized in Table II.

Averaged tensors based on single, double, triple and quadruple combinations of these rotations considered in all permutations which preserve γ as time independent were calculated.[5] Only two of these combinations predicted spectra in agreement with those observed experimentally. The first combination (A) of motions consisted of a fast rotation about the P-O11 bond, followed by a slower rotation about the glycerol C1-C2 bond, followed by a yet slower rotation about the molecular z axis. The second possible combination (B)

[4] Recent work by R. G. Griffin (private communication) has shown that the orientation of the plane containing P and the nonesterified O's is oriented approximately 50 ± 5° to the bilayer normal in a sample of oriented dipalmitoylphosphatidylcholine. This is within 5° of the orientation of this plane determined from the crystallographic data and supports the use of the crystallographic orientation in the present analysis.

[5] For example, if rotations are considered in the order R2, R1, R3 (in the notation of Table II), the angle γ between R1 and R3 is time dependent. Such combinations were not considered.

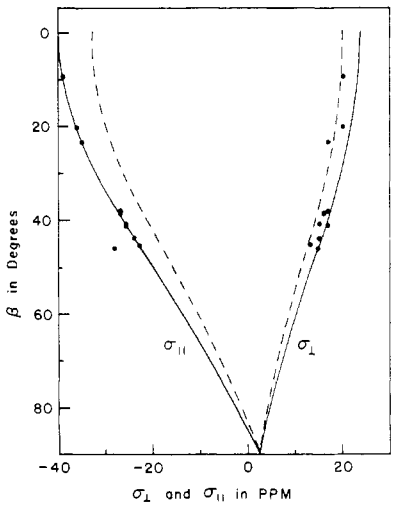

FIGURE 7: Predicted values of $\sigma_\parallel$ and $\sigma_\perp$ as a function of wobble of the molecular z axis about the bilayer normal. β is the half-amplitude of wobble, as shown in Figure 6b. The dashed line is for model A: P-O rotation followed by C1-C2 rotation and z axis rotation. The solid line is for model B: P-O rotation followed by z axis rotation. The circles are experimental values of $\sigma_\parallel$ and $\sigma_\perp$ for DPPC and egg PC spectra observed at various temperatures. Since there is no a priori analytic relationship between wobble angle and temperature, the placement of the experimental values with respect to the theoretical curves is not obvious. A reasonable choice, shown here, locates the ordinates for the sets of experimental points by placing $\sigma_\perp$ on the curve for model B; the points were not located on the dashed curve for model A because three values of $\sigma_\parallel$ fall outside the range of the theoretical curve.

included only two rotations, a fast rotation about the P-O11 bond follwed by a slower rotation about the molecular z axis. Both models are in accord with the observations that the spectra of the head group, phosphate, and hydrocarbon regions of the phospholipid molecule collapse when oriented samples are aligned at the "magic angle", indicating that there is a motional averaging axis along the bilayer normal for all three regions of the molecule (Gally et al., 1975; Seelig and Gally, 1976; McLaughlin et al., 1975b; Seelig and Seelig, 1974b; Stockton et al., 1974).

The temperature dependence observed for $\Delta\sigma$ may be simulated if one additional type of motion is included, that of a wobble or random walk of the long axis of the phospholipid molecule within a cone about the bilayer normal as diagrammed in Figure 6b. This motion implicitly includes a rotation about the molecular z axis and further averages the tensor as the angle β defining the cone is increased, according to the equations

$$\bar{\sigma}_\perp{}^{w} = \frac{1}{2}\{U(1 + W) + V(1 - W)\} \quad (3a)$$

$$\bar{\sigma}_\parallel{}^{w} = U(1 - W) + VW \quad (3b)$$

where

$$U = \frac{1}{2}\{\bar{\sigma}_\perp{}^{R}(\cos^2\delta + 1) + \bar{\sigma}_\parallel{}^{R}\sin^2\delta\}$$

$$V = \bar{\sigma}_\perp{}^{R}\sin^2\delta + \bar{\sigma}_\parallel{}^{R}\cos^2\delta$$

$$W = \frac{1 + \cos\beta + \cos^2\beta}{3}$$

where δ is the angle between the rotation axis and the axis of the wobble. The results of this further averaging are diagrammed in Figure 7 where the values of $\sigma_\perp$ and $\sigma_\parallel$ are plotted as a function of the wobble angle β for the PC molecule. Also plotted are the experimentally observed values for DPPC and egg PC. It may be seen that the data fit best with model B including the fast P-O11 rotation followed by the rotation about the molecular z axis and a wobble about the bilayer normal. Similar results were obtained for PE (collapse from $\sigma_\perp = 20$, $\sigma_\parallel = -37$ to $\sigma_\perp = \sigma_\parallel = 1$) and for PS (collapse from $\sigma_\perp = 24$, $\sigma_\parallel = -35$ to $\sigma_\perp = \sigma_\parallel = 4$). It can be seen that a wobble angle of approximately 45° is sufficient to simulate the high-temperature spectra. This is in agreement with the earlier findings of Libertini et al. (1974) in their analysis of phospholipid motion using nitroxide labels in the acyl chain region. The wobble model is appealing because it explains the variation of $\Delta\sigma$ through the use of only one mechanism and does not require the presence of qualitatively different motions at different temperatures, as would otherwise be the case. Further, the wobble model correlates well with the observation that the phase transition reflects melting of the hydrocarbon chains. Above the transition the lamellae are more fluid and have a larger area per phospholipid (Traüble and Haynes, 1971). This might allow a sharp increase in wobble amplitude and cause a marked change in $\Delta\sigma$.

Seelig and Gally (1976) used a somewhat different approach to formulate a model of head-group motion in phosphatidylethanolamine. They assume a conformation about the C1-O11 and PO-11 bonds with fixed torsion angles which jump between $\alpha_1 = \pm 193$ and $\alpha_2 = \pm 50$, respectively. These are slightly different than the values reported in the x-ray crystallographic analysis (Hitchcock et al., 1974). Using these angles, the shielding tensor is transformed to a reference frame rotating about the C1-C2 bond, and the tensor is averaged over this rotation. Further averaging is introduced by using the order parameter for the C1-C2 bond as an empirical measure of the motion of that axis. The Seelig-Gally model is compatible with our B model in that both allow rotation about the z axis and wobble about the bilayer normal. In our model B the motion is explicitly stated while in Seelig's model it is implicit in the use of the C1-C2 order parameter. The two models differ in the head-group motion, however. Model B proposes free rotation about the P-O11 bond and assumes no rotation about the C1-C2 bond, while Seelig's model assumes free rotation about the C1-C2 axis and conformational jumps about the P-O11 bond. Both models predict very similar NMR spectra and a choice between the two is not possible based on the presently available NMR data.

The existence of these different models emphasizes the fact that the results of the motional analysis are highly dependent on the choice of initial conditions. In the particular case of head-group motion in phospholipid bilayers, the initial conditions (i.e., head-group conformation and precise orientation of rotation axes) cannot be uniquely and fully specified from the data available at the present time. The motional models, therefore, must be taken as suggestive rather than definitive until such time as the initial conditions may be unequivocally defined.

Motional narrowing is observed only if the motion is fast on the NMR time scale, as expressed by the condition $\Delta\omega\tau \ll 1$ where τ is the correlation time of the motion and $\Delta\omega$ is the initial line width in radians. The rigid lattice width is on the order of 31 krad, so the narrowing criterion requires the correlation time for the rotation about the P-O bond to be less than 32 μs. The line width after the P-O rotational averaging is 15 krad, so the correlation time for the rotation about the z axis is less than 65 μs. Similar calculations indicate that the correlation time for the wobble is less than 100 μs. Values, rather than upper limits, for the correlation times may be

measured by $T_{1\rho}$ experiments, and such experiments are now in progress.

It is apparent that a diffusion of the phospholipid molecule over the surface of the spherical lamellar particle would create a variation of the molecular longitudinal axis indistinguishable from that of the stationary wobble already considered. However, a simple calculation shows this diffusion is too slow to cause the observed narrowing. The correlation time for the diffusion or wobble must be less than 100 μs and, given a lateral diffusion constant on the order of 10^{-7} cm^2/s as measured for egg PC at 65 °C (Devaux et al., 1973), a phospholipid molecule could cover an area of 10^{-11} cm^2 in this time. This would be the surface area subtended by a 45° cone on a particle 500 Å in diameter. In order to consider a diffusion mechanism rather thana wobble mechanism, the average particle diameter would have to be 500 Å or smaller. In the lamellar dispersions the outer diameters of the particles ranged from 0.25 to 0.75 μm and even when the smaller inner layers are considered, the average diameter is much larger than the requisite 500 Å. Thus the area which could be covered by a diffusing phospholipid in the allowable time is much less than the area which must be covered for adequate averaging of the shielding tensor, and the diffusion model does not explain the observed spectra. Should the diffusion coefficient be an order of magnitude higher, this might be a plausible model.

The preliminary results from the PS/Ca^{2+} system and the chick embryo fibroblasts indicate that further ^{31}P experiments with these and similar systems should be fruitful. It is known from a variety of techniques that Ca^{2+} interacts specifically with PS. This is of biological significance due to the implication of Ca^{2+} in a variety of membrane-related processes. The spectrum of Figure 4 suggests that Ca^{2+} immobilizes a fraction of the phospholipid, perhaps by forming bridges between neighboring phosphates. A spectrum of dried powder from a Ca^{2+}/PS mixture was identical with that of a powder of PS alone, indicating that the calcium ions are not interacting in a manner which changes the chemical shielding tensor of the phosphate group.

The behavior of the PS/Ca^{2+} system is interestingly different from the behavior of a phosphatidylglycerol/Ca^{2+} system reported by Cullis and De Kruyff (1976). The two phospholipids would be expected to react similarly to the presence of Ca^{2+} since both are anionic lipids, yet broadening comparable to that seen for PS/Ca^{2+} was not observed in the phosphatidylglycerol/Ca^{2+} system in the liquid crystalline phase, and no spectrum at all was obtainable in the gel phase. Experiments are currently in progress in this laboratory to verify the phosphatidylglycerol results and clarify the differences between the two systems.

The chick embryo fibroblast spectrum was acquired in a relatively short time, indicating that this will be a technique sufficiently sensitive to study intact cell systems. It is interesting to compare the fibroblast spectrum of Figure 5 with the ^{31}P NMR spectra of muscle taken at 129 MHz by Hoult et al. (1974) and of yeast taken at 145.7 MHz by Salhany et al. (1975) in relatively narrow-band free induction decay experiments. The latter show only the narrow resonances due to the small intracellular molecules, while our wideband spectrum emphasizes the phospholipids of the cellular membranes. It is hoped that techniques such as 180–τ–90 pulse sequences will allow suppression of the narrow resonance in our spectrum so that the broad resonance will be more easily defined, and such experiments are now in progress. If this does not prove feasible, it is possible to study isolated membranes rather than the intact cells, as has been done elsewhere, or to work at higher magnetic fields where the spectral features might be more easily resolved (McLaughlin, 1975b).

Acknowledgments

The authors thank Dr. Chantal Goulon for help with the PS/Ca^{2+} experiments and Dr. Jill Hatie for preparing the chick embryo fibroblasts.

References

Bissell, M. J., Hatie, C., Tischler, A. N., and Calvin, M. (1974), *Proc. Natl. Acad. Sci. U.S.A. 71,* 2520.
Chapman, D. (1975), *Q. Rev. Biophys. 8,* 185.
Chapman, D., Williams, R. M., and Ladbrooke, B. D. (1967), *Chem. Phys. Lipids 1,* 445.
Cullis, P. R., and De Kruyff, B. (1976), *Biochim. Biophys. Acta 436,* 523.
Cullis, P. R., DeKruijff, B., and Richards, R. E. (1976), *Biochim. Biophys. Acta 426,* 433.
DeKruijff, B., Cullis, P. R., and Radda, G. K. (1975), *Biochim. Biophys. Acta 406,* 6.
Devaux, P., Scandella, C. J., and McConnell, H. M. (1973), *J. Magn. Reson. 9,* 474.
Gally, H.-U., Niederberger, W., and Seelig, J. (1975), *Biochemistry 14,* 3647.
Griffin, R. G. (1976), *J. Am. Chem. Soc. 98,* 851.
Hitchcock, P. B., Mason, R., Thomas, M., and Shipley, G. G. (1974), *Proc. Natl. Acad. Sci. U.S.A. 71,* 3036.
Horwitz, A. F., Klein, M. P., Michaelson, D. M., and Kohler, S. J. (1973), *Ann. N.Y. Acad. Sci. 222,* 468.
Hoult, D. I., Busby, S. J. W., Gadian, D. G., Radda, G. K., Richards, R. E., and Seeley, P. J. (1974), *Nature (London) 252,* 285.
Jacobson, K., and Papahadjopoulos, D. (1975), *Biochemistry 14,* 152.
Kohler, S. J., Ellett, J. D., and Klein, M. P. (1976), *J. Chem. Phys. 64,* 4451.
Kohler, S. J., and Klein, M. P. (1976), *Biochemistry 15,* 967.
Libertini, L. J., Burke, C. A., Jost, P. C., and Griffith, O. H. (1974), *J. Magn. Reson. 15,* 460.
McLaughlin, A. C., Cullis, P. R., Berden, J. A., and Richards, R. E. (1975a), *J. Magn. Reson. 20,* 146.
McLaughlin, A. C., Cullis, P. R., Hemminga, M. A., Hoult, D. I., Radda, G. K., Ritchie, G. A., Seeley, P. J., and Richards, R. E. (1975b), *FEBS Lett. 57,* 213.
Papahadjopoulos, D., and Miller, N. (1967), *Biochim. Biophys. Acta 135,* 624.
Pines, A., Gibby, M. G., and Waugh, J. S. (1973), *J. Chem. Phys. 59,* 569.
Rein, A., and Rubin, H. (1968), *Exp. Cell Res. 49,* 666.
Rouser, G., Nelson, G. J., Fleischer, S., and Simon, G. (1968), in Biological Membranes: Physical Fact and Function, Chapman, D., Ed., New York, N.Y., Academic Press, p 5.
Salhany, J. M., Yamane, T., Shulman, R. G., and Ogawa, S. (1975), *Proc. Natl. Acad. Sci. U.S.A. 72,* 4966.
Seelig, A., and Seelig, J. (1974a), *Biochemistry 13,* 4839.
Seelig, J., and Gally, H.-U. (1976), *Biochemistry* (in press).
Seelig, J., and Seelig, A. (1974b), *Biochem. Biophys. Res. Commun. 57,* 406.
Singleton, W. S., Gray, M. S., Brown, M. L., and White, J. L. (1965), *J. Am. Oil Soc. 42,* 53.
Steck, T. L., and Fox, C. F. (1972), in Membrane Molecular

Biology, Fox, C. F., Ed., Stamford, Conn., Sinauer Associates, p 27.
Stockton, G. W., Polnaszek, C. F., Leitch, L. C., Tulloch, A. D., and Smith, I. C. P. (1974), *Biochem. Biophys. Res. Commun. 60,* 844.
Stockton, G. W., Planaszek, C. F., Tulloch, A. P., Hasan, F., and Smith, I. C. P. (1976), *Biochemistry 15,* 954.
Traüble, H., and Haynes, D. (1971), *Chem. Phys. Lipids 7,* 324.
Van, S. P., Birrell, B., and Griffith, O. H. (1974), *J. Magn. Reson. 15,* 444.
Veksli, Z., Salsbury, N. J., and Chapman, D. (1969), *Biochim. Biophys. Acta 183,* 434.
Verkleij, A. J., DeKruyff, B., Ververgaert, P. H. J. Th., Tocanne, J. F., and Van Deenen, L. L. M. (1974), *Biochim. Biophys. Acta 339,* 433.

Biosynthesis of the Dimethylbenzene Moiety of Riboflavin and Dimethylbenzimidazole: Evidence for the Involvement of C-1 of a Pentose as a Precursor†

William L. Alworth,* Mary F. Dove,‡ and H. Nordean Baker§

ABSTRACT: The relative incorporations of specifically labeled pyruvate, lactate, erythritol, D-erythrose, D-ribose, and D-glucose precursors into the dimethylbenzene carbon atoms of the 5,6-dimethylbenzimidazole unit of vitamin B_{12} by *Propionibacterium shermanii* have been determined. The incorporation data provide information regarding the putative four-carbon biosynthetic unit which is involved in the formation of 6,7-dimethyl-8-ribityllumazine and which is the source of the eight dimethylbenzene carbon atoms of both 5,6-dimethylbenzimidazole and riboflavin. The relative incorporations of the labeled lactate and pyruvate precursors are not consistent with either acetoin or 2,3-butanedione functioning as the four-carbon biosynthetic unit. The relative incorporations of the labeled hexose, pentose, and tetrose precursors indicate that the observed incorporation of C-1 of the pentose into the dimethylbenzene carbon atoms does not involve metabolism to a tetrose intermediate, but occurs more directly. It is concluded that the C-1 position of a pentose precursor is involved in the formation of the putative four-carbon biosynthetic unit.

The biosynthesis of riboflavin begins with guanosine triphosphate and proceeds via a series of pyrimidine intermediates (II–IV) to 6,7-dimethyl-8-ribityllumazine (V). Riboflavin synthetase then catalyzes a condensation between two molecules of 6,7-dimethyl-8-ribityllumazine (V) to yield riboflavin and to regenerate a molecule of the 4-ribitylamino-5-amino-2,6-dihydroxypyrimidine intermediate (IV). The biosynthetic pathway in Figure 1 incorporates the recent finding of Mailänder and Bacher (1976) that in *Salmonella typhimurium* riboflavin biosynthesis begins with GTP and that the ribityl side chain of riboflavin is derived from the ribose unit of the guanosine nucleotide. Additional evidence supporting this pathway has been summarized in reviews by Demain (1972) and by Plaut et al. (1974). It is to be emphasized that the eight carbons of the dimethylbenzene moiety of riboflavin are derived from a putative four-carbon precursor that is added to IV to yield V. In the riboflavin synthetase reaction, one lumazine molecule serves as a "donor" of this four-carbon unit and is converted into another molecule of IV, while the other lumazine molecule serves as an "acceptor" for the four-carbon unit and is converted into a molecule of riboflavin. Many details of this riboflavin synthetase reaction have been elucidated, including the fact that the methyl groups attached to C-6 in V ultimately become C-6 and the methyl group attached to C-8 in the riboflavin product, as outlined (Plaut et al., 1974, and references therein).

Investigations carried out in our laboratory (Alworth et al., 1969, 1971; Lu and Alworth, 1972) and those of Renz (Renz and Reinhold, 1967; Renz, 1970; Kühnle and Renz, 1971; Renz and Weyhenmeyer, 1972) have established a biosynthetic relationship between riboflavin and the 5,6-dimethylbenzimidazole (DBI)[1] component of vitamin B_{12}. Indeed, evidence suggests that riboflavin is an obligatory intermediate in the biosynthesis of DBI (Renz, 1970; Renz and Weyhenmeyer, 1972; see also discussion in Plaut et al., 1974). The biosynthetic relationship between riboflavin and DBI permits us to interpret results obtained from investigations of DBI biosynthesis in terms of the biosynthesis of the related groups of riboflavin. In particular, the incorporation of various precursors into the dimethylbenzene moiety of DBI can be interpreted in terms of their potential to serve as biosynthetic precursors of the four-carbon unit involved in the formation of V from IV. In this paper evidence is presented which leads us to conclude that this biological four-carbon unit is derived via reactions that involve the C-1 carbon atom of a pentose precursor.

† From the Laboratory of Chemical Biology, Department of Chemistry, Tulane University, New Orleans, Louisiana 70118. *Received August 19, 1976.* This work was supported by a research grant (AM 10067) and a Research Career Development Grant to W.L.A., both from the National Institutes of Health. Preliminary accounts of portions of this work have been communicated [Alworth et al. (1969, 1970)].

‡ Portions of the described work to be submitted by M.F.D. to Tulane University in partial fulfillment of the Ph.D. requirements in Chemistry.

§ Present address: Department of Medicine, Baylor College of Medicine, Houston, Texas 77030.

[1] Abbreviation used is DBI, 5,6-dimethylbenzimidazole.